The Surface Detector System of the Pierre Auger Observatory

I. Allekotte [a], A. F. Barbosa [d], P. Bauleo [ℓ], C. Bonifazi [d], B. Civit [c], C. O. Escobar [e], B. García [c], G. Guedes [f], M. Gómez Berisso [a], J. L. Harton [ℓ], M. Healy [k], M. Kaducak [j], P. Mantsch [j], P. O. Mazur [j], C. Newman-Holmes [j], I. Pepe [g], I. Rodriguez-Cabo [i] H. Salazar [h], N. Smetniansky-De Grande [b], D. Warner [ℓ], for the Pierre Auger Collaboration [m]

[a] *Instituto Balseiro and Centro Atómico Bariloche (U.N. Cuyo and CNEA, CONICET), 8400 Bariloche, Argentina*

[b] *Laboratorio Tandar, Comisión Nacional de Energía Atómica and CONICET, Av. Gral. Paz 1499 (1650) San Martín, Buenos Aires, Argentina*

[c] *Universidad Tecnológica Nacional Regional Mendoza, Mendoza, Argentina*

[d] *CBPF, Rua Xavier Sigaud 150, Rio de Janeiro, Brazil*

[e] *Universidade Estadual de Campinas, Instituto de Fisica, Departamento de Raios Cosmicos, CP 6165, 13084- 971, Campinas SP, Brazil*

[f] *Universidade Estadual de Feira de Santana (UEFS), Av. Universitaria Km 03 da BR 116, Campus Universitario, 44031-460 Feira de Santana BA, Brazil*

[g] *Universidade Federal da Bahia, Campus de Odina, 40210-340 Salvador BA, Brazil*

[h] *Benemérita Universidad Autónoma de Puebla (BUAP), Ap. Postal J-48, 72500 Puebla, Puebla, Mexico*

[i] *Dpto. Física de Partículas, Universidad de Santiago de Compostela, 15706 Santiago de Compostela, Spain*

[j] *Fermi National Accelerator Lab., Batavia IL, U.S.A.*

[k] *University of California, Los Angeles (UCLA), Department of Physics and Astronomy, Los Angeles, CA 90095, U.S.A.*

[ℓ] *Colorado State University, Fort Collins, CO 80523, U.S.A.*

[m] *Pierre Auger Collaboration, Av. San Martín Norte 306, 5613 Malargüe, Mendoza, Argentina*

Abstract

The Pierre Auger Observatory is designed to study cosmic rays with energies greater than 10^{19} eV. Two sites are envisaged for the observatory, one in each hemisphere,

for complete sky coverage. The southern site of the Auger Observatory, now approaching completion in Mendoza, Argentina, features an array of 1600 water-Cherenkov surface detector stations covering 3000 km^2, together with 24 fluorescence telescopes to record the air shower cascades produced by these particles. The two complementary detector techniques together with the large collecting area form a powerful instrument for these studies. Although construction is not yet complete, the Auger Observatory has been taking data stably since January 2004 and the first physics results are being published. In this paper we describe the technical characteristics and performance of the Surface Detector Stations of the Pierre Auger Observatory.

Key words: Pierre Auger Observatory; high-energy cosmic rays; surface detector array; water-Cherenkov detectors

1 Introduction

Cosmic rays with energies near 10^{20} eV have been a continuing mystery since Linsley reported the first such event in 1963 [1]. As yet there are no identified sources and no convincing mechanisms for accelerating particles to these energies. Interaction with the cosmic microwave background (CMB) constrains protons of $\sim 10^{20}$ eV to come from distances not greater than about 50 Mpc [2,3]. Similarly constrained are other primaries: heavier nuclei lose energy by photo-disintegration and pair production, and photons due to pair creation [4]. Furthermore, the flux of cosmic rays at these highest energies is very low (less than one event per km^2 per century per sr), so that their detailed study requires detectors covering large areas.

The Pierre Auger Observatory was designed for a high statistics, full sky study of cosmic rays at the highest energies [5]. It utilizes an array of surface water-Cherenkov detectors combined with air fluorescence telescopes, which together provide a powerful instrument for air shower reconstruction. Energy, direction and composition measurements are intended to illuminate the mysteries of the most energetic particles in nature.

On dark moonless nights, air fluorescence telescopes record the development of what is essentially the electromagnetic shower that results from the interaction of the primary particle with the upper atmosphere. The surface array measures the particle densities as the shower strikes the ground just beyond

Email address: ingo@cab.cnea.gov.ar (for the Pierre Auger Collaboration).
URL: www.auger.org.ar; www.auger.org (for the Pierre Auger Collaboration).

its maximum development. By recording the light produced by the developing air shower, fluorescence telescopes can make a near calorimetric measurement of the energy. This energy calibration can then be transferred to the surface array with its nearly 100% duty factor and large event gathering power [6,7]. Moreover, independent measurements with the surface array and the fluorescence detectors alone have limitations that can be overcome by combining the results of their measurements.

The water-Cherenkov detector was chosen for use in the surface array because of its robustness and low cost. Furthermore, water-Cherenkov detectors exhibit a rather uniform exposure up to large zenithal angles and are sensitive to charged particles as well as to energetic photons which convert to pairs in the water volume. Their use in surface arrays was proven to be successful in previous experiments [8].

Each of the 1600 surface detector stations includes a 3.6 m diameter water tank containing a sealed liner with a reflective inner surface. The liner contains 12 000 l of pure water. Cherenkov light produced by the passage of particles through the water is collected by three nine-inch-diameter photomultiplier tubes (PMTs) that are symmetrically distributed at a distance of 1.20 m from the center of the tank and look downwards through windows of clear polyethylene into the water. The surface detector station is self-contained. A solar power system provides an average of 10 Watts for the PMTs and electronics package consisting of a processor, GPS receiver, radio transceiver and power controller. The components of the surface detector station are shown in Fig. 1.

In this paper we describe the design features and performance of the surface detector hardware. This description includes the detector tanks, liners and accessories and the pure water production, as well as the most relevant steps for assembly and deployment of the surface detectors. We conclude with an overview of the technical performance of the system. The electronics system of the surface detectors will be described in a companion paper [9].

The Southern site of the Auger Observatory, now under construction in the Province of Mendoza, Argentina, is over 85% completed. Active detectors have been recording events in a stable operation mode since January 2004 [10].

2 Design Considerations

The low event rate of the highest energy cosmic rays requires an area large enough to accumulate good statistics in a reasonable time. By covering an area of 3000 km^2 at the Southern Site, the aperture achieved with the surface array

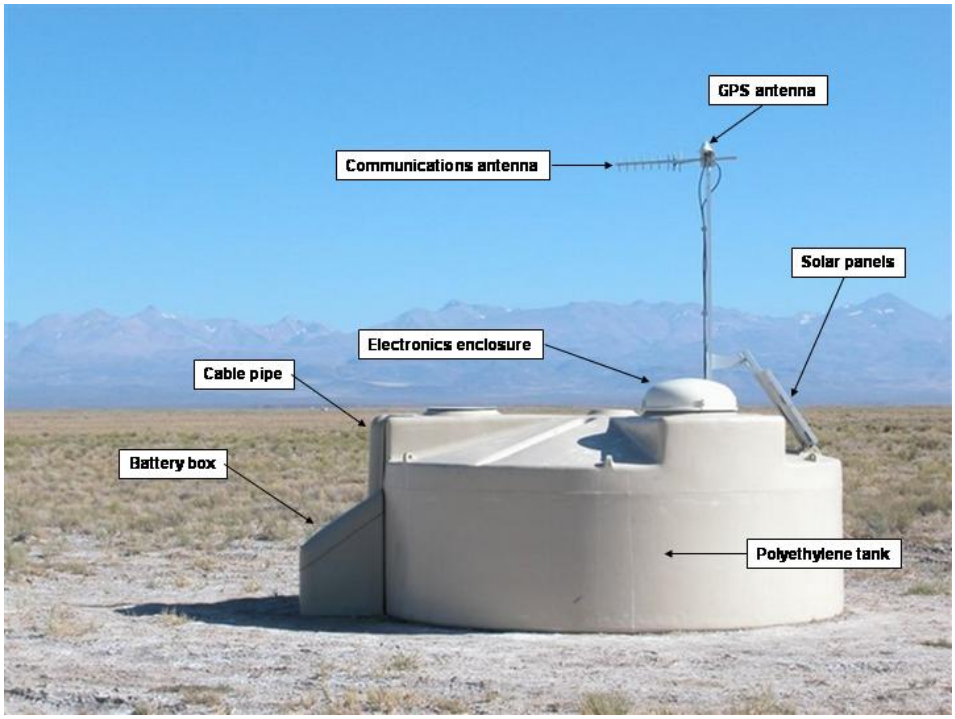

Fig. 1. A schematic view of a surface detector station in the field, showing its main components.

for zenith angles less than 60° will be 7350 km^2 sr. By including events with larger zenith angles, up to 80°, the aperture can be increased by ∼30% [11]. The detection efficiency at the trigger level reaches 100% for energies above 3×10^{18} eV [12]. This energy is determined from knowledge of the lateral distribution of showers and the single detector trigger probability, without recourse to Monte Carlo calculations. The spacing between the detector stations is the result of a compromise between cost considerations and the energy threshold (low enough to insure a good overlap with existing data.) Other important considerations are the need for sufficient sampling of the particle density away from the shower core, and the need for shower front timing in several locations. A minimum of five stations triggering at 10^{19} eV allows a maximum spacing of 1500 m on a triangular grid. At this spacing, approximately 10 stations are triggered by a nearly vertical shower with an energy of 10^{20} eV. At large zenith angles the multiplicity of stations triggered increases and at ∼60° it is typically over 20. Differential GPS systems allow the determination of position and altitude of the stations with an accuracy of less than 1 m, sufficient for a good shower reconstruction.

For the installation of this array, the site is required to be flat for good wireless communications. An altitude between 1000 and 1500 m above sea level is required for optimal development of the shower in the atmosphere. A large semi-desert area in the west of Argentina was chosen (35.0° to 35.3° S, 69.0° to 69.4° W) [13] next to the city of Malargüe . The chosen site has an average altitude of 1420 m, with detectors located at altitudes between 1340 m and 1610 m. The site has suitable infrastructure nearby as well as clear night skies and minimal light pollution which enables good fluorescence detector performance.

2.1 Energy and Angular Resolution and Composition Determination

The shower energy is obtained by determination of the signal density at a particular distance (typically 1000 m) from the shower axis. With the subset of events that the Observatory detects in hybrid mode (simultaneous measurement with both surface and fluorescence detectors), the nearly calorimetric energy determination which is possible with the fluorescence data can be used for an absolute calibration of the surface detector energy [6,7].

The signal densities measured with the surface detector array are affected by fluctuations from different origins: statistical fluctuations in the measured density, experimental uncertainties on the shower core position, incidence direction, and large physical fluctuations in the shower longitudinal development that lead to shower to shower fluctuations. The sampling fluctuations, which are dominated by the muon content of the showers, are determined by the

sampling area of the detector. At distances of around 1000 m from the shower core, the muon flux is of the order of $\sim$ 1 m^{-2} at 10^{19} eV and corresponds to roughly a half of the total signal, the other half being due to the electromagnetic component of the shower. Then, with a detector surface of 10 m^2 the sampling error in each detector is below 20%. For cylindrical detectors, this corresponds to a diameter of 3.6 m. The statistical uncertainty (including sampling and reconstruction fluctuations) in the determination of the signal density at 1000 m from the shower core is of 10% RMS for events with an energy of 5×10^{18} eV [14,15].

The direction of the primary is inferred from the relative arrival times of the shower front at different surface detectors. A weighted least squares fit is applied to the station triggering times. Fitting the station signal densities to the expected lateral distribution allows a refined core location determination. The angular resolution improves rapidly with energy and zenith angle because of the greater number of triggered stations. For the surface array alone, the angular precision is better than 1° for energies larger than $\sim 10^{19}$ eV [16–18].

The height of the water-Cherenkov detector is chosen to get a clear muon signal [19] and optimize the separation of the muon and electromagnetic contributions to the signal. A vertical height of 1.2 m of water is sufficient to absorb 85% of the incident electromagnetic shower energy at core distances larger than 100 m, and gives a signal proportional to the energy of the electromagnetic component. Muons passing through the tank generate a signal proportional to their geometric path length inside the detector and rather independent of their zenith angle and position. Each PMT collects in excess of 90 photoelectrons for each vertical muon [20].

2.2 Physical and Environmental Requirements

The Observatory will have an operating lifetime of 20 years and must be designed to survive the expected conditions at the site. The temperature ranges from -15°C to 50° with large diurnal variation. The outdoor location exposes the detectors to intense solar ultraviolet radiation and wind of up to 160 km h^{-1}. The detectors must be resistant to floods, rain, snow, dust, windblown sand and 2.5 cm diameter hail. Material selection is important because the local soils contain salts which can be corrosive to some materials. Modest seismic activity should not damage the detector units. The detector tanks must be robust and able to support a heavy person on top of the tank as well as to resist the action of insects, rodents and grazing animals.

The ground on which each detector station is placed must be leveled to prevent deformation of the tank and the area around the detector must be cleared of

heavy vegetation to avoid damage from bush fires.

2.3 Design, Development and Production Control

Each stage in the design, development and production of the surface detector station was marked by an appropriate technical review. Subsequent to the preliminary design review, 32 prototype detectors were built, deployed with standard spacing and operated in a small Engineering Array [21]. Every design feature of the detectors, the communications systems and data acquisition was tested during the two years allocated to the Engineering Array. Refinements resulting from this period were incorporated into the baseline design and subjected to a critical design review. A pre-production run of 100 detectors was then built to qualify the production process. Production readiness reviews initiated large scale component production. Assembly and deployment procedures and associated quality assurance steps were also qualified during the Engineering Array and pre-production phases.

Individual assembly steps are documented in controlled written procedures, which are also used for training and guidance of the staff. A database was developed for the traceability of detector components and the results of the tests performed on them.

3 The Tank System

3.1 Tanks

The water-Cherenkov detectors have a cylindrical shape for the water volume, which is the simplest and least expensive to manufacture. The top of the tank is rather complex in order to provide rigidity both for mounting external components such as the solar panels and for people standing on top of it, and to provide space inside the tank for the photomultiplier assemblies and cabling. The tanks do not exceed 1.6 m in height so that they can be shipped over the roads within transportation regulations. The beige tank color is selected to blend in with the natural background of the site. Although the tank liner and photomultiplier assemblies are designed for opacity to keep any external light away from the PMTs, the tank is totally opaque to provide redundancy.

For the manufacture of the surface detector tanks, the technique of rotational molding (also called "rotomolding") of high-density polyethylene was chosen for its low cost, tank uniformity and because polyethylene meets the require-

ments of robustness against the environmental elements.

In the rotomolding process, a predetermined amount of light beige powdered polyethylene is deposited inside a steel or stainless steel mold. The inside of the mold has the shape desired for the outside of the tank. The mold is closed and rotated about two axes simultaneously inside a 300°C oven. The beige powdered polyethylene melts and forms a coating on the inside surface of the mold. Heating and rotation continues until all the powder has been deposited on the surface of the mold. The rotation is briefly stopped and a predetermined amount of black powdered polyethylene is put inside the mold, which is immediately re-closed and the rotation in the oven continues until all of this powder has been deposited on the surface. Then the mold is removed from the oven and cooled while the rotation continues. Finally, the mold is opened and the tank removed.

This process, which requires between four and six hours, produces tanks with a light-beige outer layer of 1/3 of the thickness, and an opaque black inner layer guaranteeing that the tank itself will be opaque. Care in the manufacturing process results in a nearly uniform wall thickness of the desired (13 $\pm$ 3) mm and minimal warping. The nominal weight of each tank is 530 kg, varying slightly with each manufacturer. Four companies produced tanks for this project.

Lugs are molded into the tank for lifting it and for supporting the solar panels. The solar panel bracket lugs are drilled to the correct diameter after molding and access hatches are cut into the tank.

The 20-year lifetime of the tanks under outdoor conditions is a challenging specification. However, discussions with consultants and experts in the field convinced us that this can be achieved using high-quality polyethylene resins. To greatly reduce damage due to ultraviolet exposure, modern polyethylenes contain hindered amine light stabilizers (HALS). In addition, ultraviolet light is absorbed by titanium dioxide found in the beige pigment of the outer layer and by the 1% carbon black pigment of the inner layer. The polyethylene resins used for tank production are prepared in two stages. The first one is the manufacture of the base resin by polymerizing selected alkenes with suitable catalysts. This stage of manufacture also includes the addition of the light stabilizers and anti-oxidants. The character and quality of the resin are determined in this stage. The second stage is “compounding”. The polyethylene resin thus manufactured is melted and the required pigments are extruded into the resin in such a way that they mix very finely with the base polyethylene. Other additives, like HALS and antioxidants, can be mixed in at this stage as well. Then the resin is cooled and ground into a powder ready for the molding process.

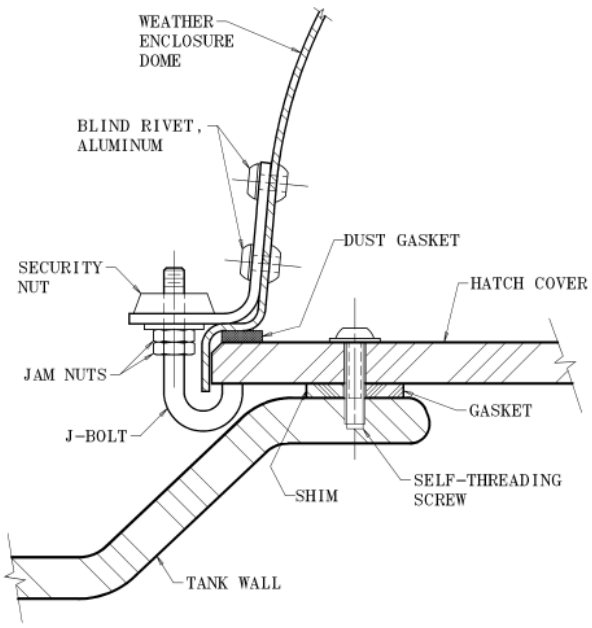

Fig. 2. Details of the hatchcover sealing system and the electronics weather enclosure dome attachment

Creep over the 20 years lifetime might also cause the tank to deform. Creep measurements of samples of our resins and extensive finite element analysis indicate that creep would not be a problem. Indeed, no evidence of either creep distortion or ultraviolet degradation have been observed in any tank, some of which have been in service for over five years.

3.2 Hatch Covers and Electronics Enclosure

As can be seen in Figs. 1 and 2, the tank hatches are elevated, to prevent rainwater from accumulating around the hatchcover and leaking into the tank.

The hatchcover assemblies for the three hatch openings (one large, 560 mm diameter, and two small, 450 mm diameter) consist of hatchcovers, gaskets, shims between the tank and hatchcover, and fastening screws. They seal and protect the tank contents, keeping out light, water and dust. They are easily removable for access to the tank contents. The large hatchcover is the mount-

ing location for the electronics and has penetrations for cable feed-throughs.

The hatchcovers are of similar material to the tank itself so that stresses in the attaching screws are minimized. Hatchcovers are machined from 12.7 mm high-density, two-layer polyethylene (HDPE) sheets with beige on the outer side and opaque black on the inner side. The shape of the hatchcover is a simple disk with 24 equally spaced holes around the outer edge for the attaching screws.

The purpose of the shim is to control the spacing between the tank top and the hatchcover at the location of the gasket, to limit its amount of compression. The shims (polyethylene) and gaskets (foam polyurethane) are bonded to the hatchcover using 3M 9472 acrylic adhesive transfer tape [1] which is particularly good at bonding to low surface energy materials, including polyethylene.

The hatchcovers are attached to the tanks using self threading screws designed for thermoplastics, identified as Plastite 48-2. The 5.3 mm diameter screws are made from stainless steel and have a tamper-resistant (pin-in-head) Torx head for increased security.

The detector electronics enclosure is mounted on the large hatchcover and protected by a weather enclosure, a dome that provides rain and dust protection and the outer security layer. The dome can be seen in Fig. 1. The dome itself is spun from 2.3 mm soft aluminum. A foam polyurethane dust gasket is installed inside the lower lip so that it compresses against the large hatchcover. The dome is painted beige to match the color of the tank. The hold-down system for the weather enclosure consists of a bracket riveted to the dome, a J-bolt which engages the large hatchcover, two jam-nuts and one security nut, which can be opened only with a special tool.

3.3 Battery Box System

Attached to the Surface Detector is a rotational molded polyethylene box containing the batteries and charge regulator for the solar power system. The battery box, visible in Fig. 1, is placed on the southern side of the tank, where the tank protects it from direct sunlight to keep the temperature low and thus increase the lifetime of the batteries. A polyethylene plate is screwed to the bottom of the box and extends below the tank to anchor the box, deterring theft or displacement by large animals. The box has a rounded back with radius of curvature equal to the tank radius to fit close to the tank. The corners of the box are rounded to discourage rubbing by cows. The interior of the box is lined with 50 mm polystyrene foam sheets as thermal insulation.

[1] 3M, St. Paul, Minnesota, U.S.A., www.3m.com

The top of the box has a slope to deter its use as a step to get on the tank. The lid is held on with security-head screws. A protective cover is mounted to the tank to shield the power system cables that run from the inside of the tank, above the water level, to the interior of the battery box.

4 Solar Power System

4.1 Solar panels and batteries

Power for the electronics is provided by a solar photovoltaic system. The power system provides the required 10 W average power. A 24-V system has been selected for efficient power conversion for the electronics.

Using the available insolation data for the Auger site, it was found that a suitable power system can be obtained with two 55 Wp panels [2] and two 105 Ampere-hour (Ah), 12 V batteries. Power is expected to be available over 99% of the time. Even if after long-term operation the capacities of the solar panels and batteries are degraded to 40 Wp and 80 Ah, respectively, power would be available 97.8% of the time.

The batteries [3] selected for the project are a new type of lead acid battery designed for solar power applications. They have a selectively permeable membrane and do not require maintenance. Other lead-acid battery technologies are being considered for replacement batteries as these wear out.

The charge controller [4] was selected for robust design and construction, to maximize the lifetime expectations. An encapsulated, epoxy potted model with robust surge protection was found in the solar power market. The controller is pulse width modulated and operates by applying pulses of current of varying width to the batteries, as their state of charge varies with battery voltage and temperature. This is considered to be the best method of charging for maintaining battery efficiency and lifetime. There have been no observations of electronics interference arising from the charge controller.

[2] Wp is a unit expressed in watts for solar panel output with a standard solar irradiation applied.
[3] Model 12MC105, Acumuladores Moura S.A., Brazil, www.moura.com.br
[4] Sunsaver SS-10-24V, Morningstar Corporation, U.S.A., www.morningstarcorp.com

4.2 Solar Panel Support Brackets and Masts

The solar panel bracket supports the solar panels and includes the mast that supports the communications antenna and the GPS antenna. The bracket system is designed to withstand 160 km h^{-1} winds.The brackets are built using aluminum 38 mm square tubing with aluminum blind rivets, and the aluminum alloys used were selected for good corrosion resistance. The brackets are prepared by cutting, drilling and riveting most of the assembly in a factory. A few of the rivet holes are not drilled until the bracket is test-fitted to the tank, so that the variability in the dimensions from tank to tank is compensated for. The assembly of the solar panels to the brackets and of the brackets to the tank is completed before the detectors are taken out into the field, but the brackets are left in a collapsed configuration for ease of transportation. When the detector is in its final position the panels and mast are raised and locked in place by a single bolt.

4.3 Power Cabling

By mounting the electronics directly on the hatchcover, the length of cables and the number of connections and feed-throughs are minimized. The power cables run from the solar panels to the electronics enclosure and from there through the interior of the tank to the battery box. They penetrate the large hatchcover and the tank with light- and water-tight cable feedthroughs. The only cables exposed to the outside world are the two antenna cables and the solar power cable coming from the bracket assembly and entering the electronics enclosure. They are UV protected for outside use. Heavy gauge wiring was selected for robustness rather than for electrical resistance considerations.

Sensor cables are installed with the power cables. Voltage of the individual batteries, their charge and discharge current as well as the temperatures of the batteries and the bases of the PMTs are monitored and registered in 6-minute intervals. The monitoring of the batteries is also required as the tank power control board is designed with the capability of setting the local station in hibernation mode if the voltage drops too low after many days without sunshine. After a period of prolonged cloudiness, all stations of the array can be shut down simultaneously rather than shutting down individual stations, minimizing recovery times and maximizing data integrity. Power system connectors are automotive grade, gold-plated for long durability in the harsh field conditions.

A grounding rod is driven into the ground at the opening between the battery box and the tank and connected to the negative terminal to provide the

electronics system grounding.

5 Liners

5.1 Development and Design

Tank liners are right circular cylinders made of a flexible plastic material conforming approximately to the inside surface of the tanks. The liners fulfill three functions: they enclose the water volume, preventing contamination or the loss of water and providing a barrier against any light that enters the closed tank; they diffusively reflect light traversing the water; and they provide optical access to the water volume for the PMTs, such that PMTs can be replaced without exposing the water to the environment.

The liners also must not contaminate the pure water themselves. Three dome windows and five fill ports with screw caps are hermetically sealed to the liner. The window assemblies allow for the mounting of the PMTs. The fill ports allow for filling and venting the tank, as well as providing a window for an LED flasher used for initial testing.

Although the tanks provide the primary light barrier for external light sources, it is necessary that the liners be completely opaque to act as a secondary protection against small light leaks. Initial tests were performed to ensure that the laminate and the seals are completely opaque against single-photon level light transmission, i.e., a 0% light transmission for light of wavelengths between 300 and 700 nm, as measured by counting single-photon detection rates.

Although the mass of water moderates temperature fluctuations, the temperature range to which the liner is exposed is from nearly -10°C to +50°C. Up to 10 cm of ice could form at the upper surface or sides of the water volume. The liner is designed to be sufficiently strong and flexible that it is not damaged by such ice formation. Ice is prevented from forming near the PMT windows by mounting insulating rings of polystyrene foam. Strength and flexibility are also required to withstand the formation of waves up to 15 cm high on the surface of the water produced by eventual seismic activity. The Observatory is located in an area rated for moderate seismic activity and the detector was designed to resist damage from such activity.

Liner materials require strength, opacity to external light, diffuse reflectivity of inner surface, sealability, resistance to chemicals from the environment and to biological activity and minimal extractables from the material which might

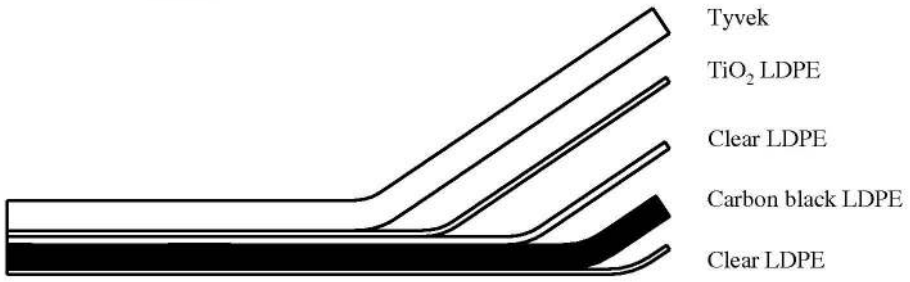

Fig. 3. A sketch of the laminate, showing the outer Tyvek® layer, the medium TiO_2 LDPE layer and the 3-layer with clear LDPE, LDPE with carbon-black and clear LDPE.

contaminate the water volume enclosed.

The liners are produced from a laminate composed of an opaque three-layer co-extruded low-density polyethylene (LDPE) film bonded to a 5.6 mils thick layer of Dupont Tyvek® 1025-BL [5] by a layer of Titanium-dioxide pigmented LDPE of 1.1 mils thickness (see Fig. 3). The three-layer co-extruded film consists of a 4.5 mils thick carbon black loaded LDPE formulated to be opaque to single photons, sandwiched between layers of clear LDPE to prevent any carbon black from migrating into the water volume. The LDPE was metallocene catalized linear low-density polyethylene (LLDPE) with excellent strength and flexibility. Tyvek® 1025-BL was chosen as the reflective layer due to its strength and excellent diffuse reflectivity for Cherenkov light in the near ultraviolet [22,23]. Tyvek® 1025-BL is an untreated polyolefin non-woven material,

[5] E.I. du Pont de Nemours and Co., Wilmington, Delaware, U.S.A., www.dupont.com

which minimizes the chemicals available to leach into the water volume. It is the thinnest of the "biological grade" Tyvek® commercially available, which simplifies the bonding processes used in manufacturing liners.

Polyolefin film has a strong tendency to pick up electrostatic charge when unrolled or pulled over a surface and even in a very clean assembly environment would collect significant dust during the hours involved in liner assembly. The method for controlling contamination of the liners centers on minimizing food sources for microbes by eliminating hair and skin contact with the lamination and working in a reasonably clean environment. Although the Auger lamination is not produced in a "clean room" environment, the extruders, lamination machines and slitting machines are all cleaned prior to production of the Auger lamination, and hair restraints and gloves are worn during all handling of the film.

5.2 Assembly and Testing

Liners are assembled by first manufacturing three separate sections of laminate and then sealing them together. The separate sections are the bottom, side strip, and top. The liner top is the most complex section since it includes the PMT and LED windows and fill/vent ports. Seals are made by welding the layers together under pressure with custom designed impulse heat seal machines. The liner tops were assembled using the same cleanliness procedures as for laminate manufacture mentioned above. Final liner assemblies were done in a class 100 000 clean room specially set up for this project.

All liners were tested for leaks and flaws, and any defects were repaired before packing and shipping to the site. The same tests were repeated at the assembly site prior to installation.

For testing, the liner is inflated to a pressure of 20 millibar over atmospheric pressure, see Fig. 4. Then all the seals are tested using a soap bubble solution, looking for visible signs of bubbling. The liner is then examined in a darkened room with bright lights covering the window ports such that they only illuminate the interior of the liner. Any visible light leaking out from the liner indicates a fault requiring repair. The testing procedures described above were determined to be sensitive to leaks smaller than those which could cause a loss of 10% of the detector volume in 20 years.

Fig. 4. An inflated liner during testing.

5.3 Dome Assembly and PMT Enclosure

The PMT enclosures have been designed to allow the PMT to collect Cherenkov light from the water detector volume while providing for a cover to shield the PMT from external light and protecting it from the external environment (see Fig. 5).

The foundation of the PMT assembly is an annular, LLDPE flange that is heat-sealed directly to a hole in the top of the liner using a custom circular heat impulse welder. The window through which the PMT views the water is made of UV-transparent LLDPE. The windows are vacuum formed to fit approximately the nominal PMT face. The window is heat sealed to the flange. Using heat seals rather than any adhesive insures that the only material in contact with the water is polyethylene. The PMT is protected on the top from light by an injection-molded ABS plastic cover called the "fez". For installation the PMT is indexed with respect to the fez using an internal polystyrene foam collar that is bonded to the PMT neck. The variance in the PMT face shape results in a few millimeters uncertainty on the space between the window and the PMT face, and that space is filled with 150 ml of the silicone optical compound GE6136 RTV[6]. Without the optical coupling approximately half the light from the tank is lost due to total internal reflection and direct reflection from the interfaces. The fez, with PMT in place, is sealed to the flange using black GE 123 RTV[6] at the time that the optical seal is made. The fez has four ports. One port is a light-tight air vent to prevent pressure buildup due to temperature changes. The other three ports are for cable feed-throughs. These are custom molded two-piece parts (identical left and right parts) that clip around the cables and clip to flat annular regions on the fez. There are similar feed-throughs to pass cables through the bottom of the hatch cover into the electronics enclosure. Finally there are two annular polystyrene foam insulation pieces that fit inside the fez to prevent ice buildup near the PMT. One insulation piece is the same one that fits on the PMT neck to fix its position with respect to the fez. The other fits at about water level and fills the space between the inside of the flange and the top of the bulb of the PMT glass. Tests show that ice will form in extreme years on the water surface, but with the insulation in place it will not stress the optical coupling or the PMT itself.

[6] General Electric Company, U.S.A., www.gesilicones.com

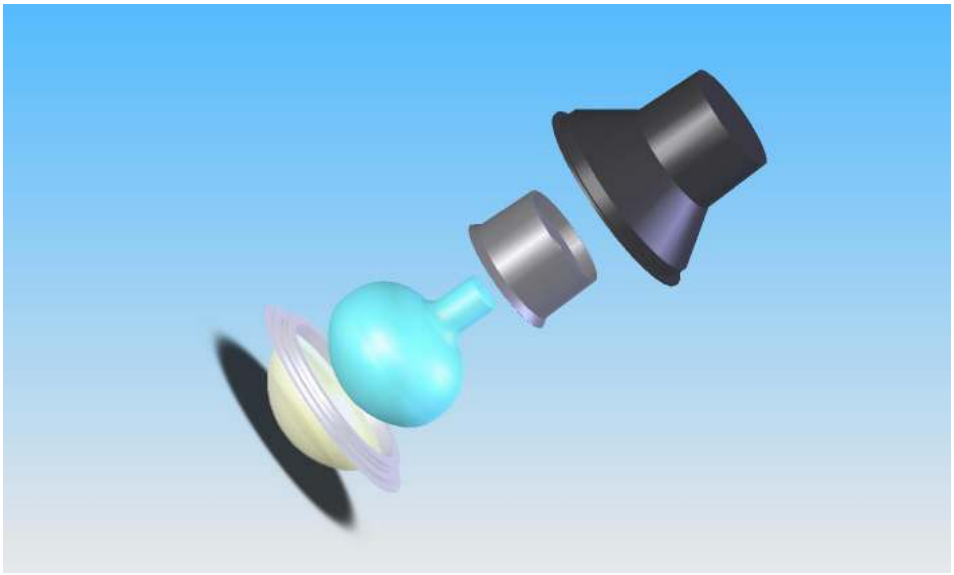

Fig. 5. Mechanical housing for the PMT (top to bottom): Outer ABS plastic housing; insulating plug affixed to the PMT neck that centers the PMT and sets the distance of the PMT face to the window; PMT; flange to which the housing is glued with a room- temperature RTV; UV-transparent window which is fixed to the PMT using a UV-transparent optical coupling.

6 Water

6.1 Water Quality Specification

Each surface detector contains 12 000 l of ultra-pure water. The high water purity is required for two purposes: to achieve the lowest possible attenuation for UV Cherenkov light, and to guarantee stability of the water during the 20 years of operation of the detectors.

For these reasons, the detector water needs to be deionized and completely free of microorganisms and nutrients. After consulting experts in pure water production, it was established that the best achievable water quality requires a water treatment that gives an output water of resistivity above 15 MΩ-cm.

The production rate of the water plant has to be high enough to ensure that it can provide water to the detectors at the same rate as they are deployed. This requirement corresponds to up to 36 000 l/day, which would allow us to fill up to 90 detectors per month.

6.2 Water Production

The pure water required for the surface detectors is produced at a plant owned and operated by the Auger Observatory and installed at the Central Campus in Malargüe.

Water is provided both from a local well at 80 m depth and from the city of Malargüe water network and pumped to a cistern with 60 m^3 capacity where it is chlorinated and stored. The water plant is fed from this cistern. As the quality of the city water is considerably better than the underground water but more expensive, the admixture allows an increased production rate and reduced contamination in the effluents at the lowest cost.

The water purification follows four stages:

(1) Pre-processing:
- Prefiltering, to eliminate particles greater than 40 μm.
- Softening with a resin bed for strong cationic exchange, with regeneration by sodium chloride, to eliminate Ca^{++}, Mg^{++} and Fe ions.
- Addition of antiscale solution, to avoid deposit of silicates on the reverse osmosis membranes (see below).
- Addition of chlorine reducer to eliminate active chlorine.
- Microfiltering with two pairs of polypropylene microfilters to eliminate

particles greater than 5 μm.

- Ultraviolet disinfection with a 254-nm UV unit (64 W power), to eliminate microorganisms from the water.

(2) Reverse osmosis: A high-pressure centrifugal pump pressurizes the water and pumps it to the reverse osmosis unit, consisting of two modules in parallel with 4 membranes each and, in series at their output, a third module with 4 membranes. Maximum input flow is 4500 l/h, with a maximum output of 2800 l/h. The output water resistivity is $\sim$ 100 kΩ-cm.

(3) Ultraviolet purification: an ultraviolet source of 185 nm eliminates microbiological residues and removes Total Organic Carbon (TOC).

(4) Continuous Electrodeionization (EDI): To achieve the required final water quality (resistivity above 15 MΩ-cm), the product of the reverse osmosis process is fed to an EDI unit [7], which consists of a set of membranes with cationic and anionic transfer. The production capacity of this unit is up to 3400 l/h.

The high-purity output water is stored in a 50 000 l storage tank. A recirculation system, which also permits quality improvement through a mixed resin bed and UV treatment (254 nm, 151 W), can recirculate up to 5 500 l/h. The pumping system of this recirculation is also used to fill the transport tank.

The water plant is fully automated. Instruments monitor the working parameters of the water plant: a chlorine monitor at the entrance of the reverse osmosis membranes, pressure gauges, flux gauges, flow meters and resistivity meters. A programmable logical controller (PLC) records the relevant production parameters.

6.3 Water Testing and Handling

The two most relevant parameters that give information about water quality are its resistivity and biological activity. Resistivity can be measured continuously at the output of the water plant and in the storage tank with the instruments incorporated at the water plant. Resistivity of the water in the transport tank and in the detectors is determined with hand-held conductivity meters. Although the water resistivity degrades during transportation, probably due to absorption of carbon dioxide, tanks in the production phase are filled with water of 8 to 10 MΩ-cm. During the initial phases of the project, Engineering Array tanks were filled with water of less than 1 MΩ-cm quality and they worked as required for nearly 4 years [21].

The TOC, i.e., potential nutrients for bacteria, is removed by the short wave-

[7] Model E-Cell MK-1 PHARMA, General Electric Company, U.S.A., www.gewater.com

length UV exposure followed by deionization. The plant manufacturer specifies that 10 ppb should be achieved. It is not feasible to measure TOC in the tanks deployed in the field with the required accuracy, so TOC was only measured a few times at the output of the water plant, yielding values below 100 ppb.

To determine the biological activity in the water, samples are taken periodically from the storage tank, the transport tank and the detectors themselves. These samples are kept in a sterile container and sent to a biochemists' laboratory to perform the corresponding analysis and search for aerobe mesophylls, coliforms, faecal coliforms, coliforms in Koser citrate, yeasts and fungi in Agar Saboreaud medium. In most of the cases, no biological activity has been found. Some isolated tanks showed contamination with low quantities of aerobe mesophylls, identified as being of the genus "Serratia", which might originate from contamination during sampling or during sample transportation. In all cases, the initially detected bacterial contamination was low (below 2000 colony forming bacteria per ml) and these tanks were monitored periodically and in no case could a large or steady increase in bacterial activity be detected.

6.4 Long-Term Stability

The long-term trends in water quality are tracked using the on-line tank calibration and monitoring system that is active for every station and updates every four hours [20]. In this application, the time structure of the collected Cherenkov light produced by through-going muons is recorded to measure the water purity indirectly [24]. Use of the calibration and monitoring system has the advantage that every station in the array can be followed and the great quantity of data collected allows some predictive power even if the measurement lacks the directness of water sampling.

The charge registered in the fast analog-to-digital converter from single muons rises rapidly, peaks, and then decreases exponentially. The decay time depends on the rate of Cherenkov light absorption and on the reflectivity of the interior of the liner. Measuring the time constant quantifies the amount of Cherenkov light that is absorbed in a way that is largely unrelated to the absolute photoelectron count. An absolute photon count depends on more than just the amount of absorption in a station. Although it is possible to fit the muon traces directly and obtain the time constant, this method is dependent on the precise details of the fitting procedure. For this reason Q_{VEM} (the total charge deposit by a vertical muon) divided by I_{VEM} (the signal maximum for a vertical muon) is used as a substitute for the actual time constant. That ratio can then be examined as a function of time to search for trends that have time scales in the range of a few months to several years.

Application of this technique allowed us to observe a decline by 10% in the Q_{VEM}/I_{VEM} ratio in the first several months after deployment, at which time it reaches an equilibrium. The origin of this behaviour is still under investigation. After this the water quality is nearly constant with a small annual oscillation of less than 1% in the Q_{VEM}/I_{VEM} ratio, linked to seasonal changes.

7 Detector Assembly and Deployment

7.1 Detector Assembly

The assembly of the surface detector stations is done in the Assembly Building located at the Central Campus of the Observatory in Malargüe. The different components are received and assembled into a complete detector in this building, which provides workspace for eight detectors at a time.

When received, tanks are unloaded and inspected. Using a template, holes are drilled to guide the hatchcover screws and the hatches are closed to keep water and dirt out of the tank during outdoor storage. Dimensional measurements, including ultrasonic measurements of the tank wall thickness, are performed to ensure tank quality. After cleaning, the tank interior is checked for imperfections that could damage the liner. Holes for venting, water drain and cable feed-throughs are drilled into the tank, cables are passed through the interior of the tank and the liner is inserted and inflated with filtered air. PMTs are installed and glued to the liner window domes using optical RTV. Fezzes are mounted over the PMTs to ensure a light-tight seal. The remaining items are mounted to the tank: the half-pipe to protect the cables running outside the tank, the solar panel brackets with solar panels and the electronics enclosure dome. The liner is kept inflated with air for safe transportation to the field, and foam pads are inserted between the PMT fezzes and the hatchcovers to provide cushioning of PMTs during transportation. Six full time technicians, one foreman and an administrative assistant (for data entry, inventory and parts receiving and management) can assemble eight tanks every two days. This includes the assembly of the solar panel brackets and the preparation of the battery boxes. PMTs are tested in the Assembly Building after installation, and serial numbers of the main detector parts are recorded and entered into the parts management database.

Detector deployment involves survey and site preparation, delivery of the detector units to their prepared locations, delivery of water and installation of the components necessary to complete the detector. The main challenge for deployment is transportation over difficult and variable road conditions, particularly with heavy loads of water. Access to detector locations is affected by

seasonal and daily weather conditions.

7.2 Site Survey and Preparation

Prior to detector deployment, the ground for each surface detector location is prepared following these steps:

- A contract surveyor marks the location where each detector is to be deployed with two stakes oriented north-south at a distance of roughly 10 m from each other. The surveyor provides the Project with information on the positioning of both stakes (including altitude) with centimeter precision, as well as information on ground conditions.
- A circular area of 6 m radius is cleared of vegetation. At locations with pampas grass ("cortadera") or heavy brush, the circular cleared area is increased to 10 m radius to reduce the seasonal fire hazard. Local environmental regulations and procedures are observed.
- A central circular area of 2.5 m radius is prepared by clearing it of stones, roots and other sharp objects and irregularities to avoid damage to the tank bottom. the ground is leveled to within 3 cm to avoid overloading the walls of the detector tank and to provide a uniform water depth and PMT height.

The aim was to place all of the detectors on a hexagonal grid of 1500 m spacing. However, for practical reasons, deviations from this ideal have been inevitable although the median location is within 12 m of the optimum position. Only 4% of the detector positions are more than 50 m away from the ideal location, with 0.4% of the detectors being displaced more than 100 m. These large displacements (which have little impact on reconstruction accuracy) were necessary because of a cultivated area, a riverbed or a swamped and inaccessible area.

7.3 Deployment

The deployment procedure starts with loading assembled tanks and transporting them to a staging area at the site. Tank transport to the staging area is done with flatbed tractor-trailer trucks carrying four tanks at a time. Staging areas are selected to be approximately equidistant from the four deployment locations and in an area where the truck transporting the tanks can easily maneuver. An escort vehicle carries other components for deployment.

Loading at the Assembly Building is done with a forklift truck. All tank lifting is performed using the lifting lugs molded into the top of the tanks along with clevises and straps. Unloading and further transportation at the site requires

a truck capable of carrying a single tank and equipped with a hydraulic crane. Such trucks are commonly used for transporting bricks, drywall, roofing materials and other construction supplies. While being unloaded and positioned, the tank is oriented such that the solar panel will face north (5° tolerance) as determined with a compass. Once the tank is positioned, the battery box is installed at the south side of the tank and batteries and charge regulator are installed and connected.

Water is delivered to the detector as discussed in the following section. During water filling, the water delivery team installs the communications antenna kit and the GPS antenna and mounts them to the mast.

Finally, installation of the electronics kit is performed by a team of two electronics technicians. The electronics for the detector station are tested and the detector is commissioned. Contact via a mobile radio system to a data acquisition technician at the Central Campus allows the deployment technician to check that the detector is performing correctly and sending triggers to the central data acquisition system at the Central Campus before leaving the field. At this stage the detector is fully integrated into the data taking system.

7.4 Water Delivery

Water is delivered to each detector tank (12 000 l) in one filling, with a single hose connection. Only a single connection is used in an effort to prevent contamination by bacteria and/or potential nutrients.

A water delivery system is composed of two 12 500 l tanks, one mounted on the back of a truck and one mounted on a trailer. Each tank has an electrically powered pump, a gasoline powered generator, hoses, connections and accessories. The trailer is pulled by the truck on easy access roads and tracks. To access the more difficult areas, the trailer or the truck are pulled by a large front-end loader. The front-end loader is also used to even out irregular roads and to compact the ground in wet areas.

The transport tank system has the following characteristics:

- The first transport tank that was acquired for water delivery was made of fiberglass-reinforced polyester resin with food-grade protective coatings on the inside. The maximum allowable working differential pressure of the tank is 100 cm of water. For full scale deployment, three additional tanks were purchased, made of stainless steel (AISI 304 with 2-b sanitary finishing) as this is more robust to damage in the harsh field conditions and can be kept clean more easily. Two of these tanks were mounted on trucks and two on trailers.

- A 0.2 μm bacteriological filter is connected to the air inlet of the tank to filter the air that is sucked into the transport tank as the water is pumped out. A valve is installed below the filter, to ensure that the water cannot splash the filter during truck movements because the filter has a very high pressure drop when wet. The valve is opened when the tank is being emptied to allow inflow of air.
- Each tank has a manway to allow access for cleaning. A pressure relief valve is installed at the manway to avoid damage to the tank by overpressure during filling.
- There is a transparent plastic window on the tank for direct visual inspection.
- A 50 mm hose and associated valves are installed to transfer the water from the transport tank to the detector. The end of the hose is connected to a bayonet that has a valve to regulate water flow and a freely rotating cap that can be screwed to the liner opening. During transportation, the bayonet is protected with a stainless steel scabbard which can be screwed to the bayonet with an airtight seal.
- The electrically driven stainless steel centrifugal pump installed to transfer the water has a capacity of 120-300 l min^{-1}.
- All accessories in contact with water are stainless steel with a sanitary finish to prevent corrosion and formation of bacterial colonies.

The recirculation system of the water plant is used to fill the transport tank. This allows a flow of 12 500 l in 50 minutes. Before filling the tank the water conductivity is tested with a hand-held conductivity meter. To fill the detectors, hatch covers are removed after cleaning the tank surface, one liner cap is opened and the bayonet, after being rinsed thoroughly, is introduced into the liner and screwed to the liner opening, and the pump is turned on. A second liner port is opened for air release. The filling of the detector takes approximately 45 minutes. The height of the water column is determined by measuring the height of the tank and subtracting the height of the water level, measured from the top of the tank. This gives a precision of 1-2 cm. The level is measured at different hatch openings to avoid systematic errors due to any possible tank tilt. After filling, any remaining air is pumped out of the liners with a vacuum cleaner. Once deployed, water level measurements can be obtained from the slope of the charge histogram from single muon tracks [25,24].

After pauses in water deployment of five to six days, the transport tanks and all accessories are cleaned and disinfected, and filters are checked and replaced as required. Cleaning is done with detergent, bleach and a very thorough rinse.

8 Performance and Conclusions

8.1 Performance, Maintenance and Operation

As of July 2007, more than 1300 surface detector stations are operational. Typically more than 98.5% of the stations are operational at any time. The technical staff distributes its time between deployment of new detectors and maintenance and repair of down stations.

Only seven liners were observed to leak shortly after installation. In these cases, which constitute the worst failure mode, the tank is emptied and brought back to the Assembly Building for replacement of the interior components.

There have been very few instances of human interference with the surface detectors. During 5 years of operation, only 12 solar panels have been damaged and two have been removed (both from locations along side a paved road).

Solar power system parameters are recorded and analyzed using the central data acquisition system. Failures are treated on an individual basis. Monitoring software for the solar power system has been developed to make this monitoring routine for operating personnel and scientists either on shift at the site or elsewhere by internet access. The lifetime of batteries is estimated to be four years. The batteries will be monitored along with the rest of the solar power system. The condition of the batteries can be determined from the data (voltages, currents, and temperatures) that are being monitored and the weak batteries can therefore be identified weeks or even months before complete failure occurs. Batteries can then be scheduled for replacement by the routine maintenance process.

In conclusion, with over 1300 commissioned detectors in the field, some of which have already been operational for over five years, much insight on their performance has been gained. All components of the above-described detector hardware have fully met our design expectations. The design has proven sufficiently robust to withstand the adverse field conditions and failure rates are less than expected. Data taking is ongoing and the first scientific results have already been published. The physics performance has met or exceeded all of our requirements.

Acknowledgements

The successful installation and commissioning of the Auger Surface Array would not have been possible without the strong commitment and effort from the technical and administrative staff in Malargüe.

We are very grateful to the following agencies and organizations for financial support: Gobierno de la Provincia de Mendoza, Comisión Nacional de Energía Atómica, Municipalidad de Malargüe, Fundación Antorchas, Argentina; the Australian Research Council; Fundação de Amparo a Pesquisa do Estado de São Paulo, Conselho Nacional de Desenvolvimento Científico e Tecnológico, Fundação de Amparo a Pesquisa do Estado de Rio de Janeiro and Financiadora de Estudos e Projetos do Ministerio da Ciencia e Tecnologia, Brasil; Ministry of Education, Youth and Sports of the Czech Republic; Centre National de la Recherche Scientifique, Conseil Régional Ile-de-France, Département Physique Nucléaire et Corpusculaire (PNC-IN2P3/CNRS), Departement Sciences de l'Univers (SDU-INSU/CNRS), France; Bundesministerium für Bildung und Forschung, Deutsche Forschungsgemeinschaft, Helmholtz-Gemeinschaft Deutscher Forschungszentren, Finanzministerium Baden-Württemberg, Ministerium fr Wissenschaft und Forschung Nordrhein Westfalen, Ministerium für Wissenschaft, Forschung und Kunst Baden-Württemberg, Germany; Istituto Nazionale di Fisica Nucleare and Ministero dell'Istruzione, dell'Universitá e della Ricerca, Italy; Consejo Nacional de Ciencia y Tecnología Mexico; Ministerie van Onderwijs, Cultuur en Wetenschap, Nederlandse Organisatie voor Wetenschappelijk Onderzoek, Stichting voor Fundamenteel Onderzoek der Materie, Netherlands; Ministry of Science and Higher Education, Poland; Fundação para a Ciência e a Tecnologia, Portugal; Slovenian Ministry for Higher Education, Science, and Technology and Slovenian Research Agency; Comunidad de Madrid, Consejería de Educación de la Comunidad de Castilla La Mancha, FEDER funds, Ministerio de Educación y Ciencia, Xunta de Galicia, Spain; Science and Technology Facilities Council (formerly PPARC), UK; the US Department of Energy, the US National Science Foundation, The Grainger Foundation, U.S.A.; UNESCO and the ALFA-EC in the framework of the HELEN Project.

References

[1] J. Linsley, Phys. Rev. Lett. **10**, 146-148 (1963)

[2] K. Greisen, Rev. Lett. **16**, 748 (1966)

[3] G.T. Zatsepin, V.A. Kuz'min, JETP Letters **4**, 78 (1966)

[4] M. Nagano, A.A.Watson, Rev. Mod. Phys. **72**, 689 (2000)

[5] Pierre Auger Observatory Design Report (March 1997), www.auger.org/admin

[6] The Pierre Auger Collaboration, "First Estimate of the Primary Cosmic Ray Energy Spectrum Above 3 EeV from the Pierre Auger Observatory", Proceedings of the 29th International Cosmic Ray Conference, Pune, India, **7**, 387 (2005)

[7] M. Roth for the Pierre Auger Collaboration, "Measurement of the UHECR energy spectrum using data from the Surface Detector of the Pierre Auger Observatory", Proceedings of the 30th International Cosmic Ray Conference, Merida, Mexico (2007), H.E. 1.4.A - 313. arXiv:0706.2096v1 [astro-ph]

[8] M.A. Lawrence, R.J.O. Reid and A.A. Watson, J. Phys. G **17**, 733 (1991)

[9] T. Suomijarvi et. al. for the Pierre Auger Collaboration, "The Electronics System of the Surface Detectors of the Pierre Auger Observatory", in preparation

[10] T. Suomijarvi for the Pierre Auger Collaboration, "Performance of the Pierre Auger Observatory Surface Detector", Proceedings of the 30th International Cosmic Ray Conference, Mérida, Mexico (2007), H.E. 1.4.A - 299. arXiv:0706.4322v1 [astro-ph]

[11] P. Facal San Luis for the Pierre Auger Collaboration, "Measurement of the UHECR spectrum above 10^{19} eV at the Pierre Auger Observatory using showers with zenith angles greater than 60°", Proceedings of the 30th International Cosmic Ray Conference, Mérida, Mexico (2007), H.E. 1.4.A - 319. arXiv:0709.1823v1 [astro-ph]

[12] D. Allard et. al. for the Pierre Auger Collaboration, "Aperture calculation of the Pierre Auger Observatory surface detector", Proceedings of the 29th International Cosmic Ray Conference, Pune, India, **7**, 71 (2005)

[13] I. Allekotte et. al, J. Phys. G: Nucl. Part. Phys. **28**, 1499 (2002)

[14] P. Ghia for the Pierre Auger Collaboration, "Statistical and systematic uncertainties in the event reconstruction and S(1000) determination by the Pierre Auger surface detector", Proceedings of the 29th International Cosmic Ray Conference, Pune, India, **7**, 167 (2005)

[15] M. Ave et. al. for the Pierre Auger Collaboration, Nucl. Inst. & Meth. **A578**, 180 (2007)

[16] C. Bonifazi for the Pierre Auger Collaboration, "Angular Resolution of the Pierre Auger Observatory", Proceedings of the 29th International Cosmic Ray Conference, Pune, India, **7**, 17 (2005)

[17] M. Ave for the Pierre Auger Collaboration, "Reconstruction accuracy of the surface detector array of the Pierre Auger Observatory", Proceedings of the 30th International Cosmic Ray Conference, Merida, Mexico (2007), H.E. 1.4.A - 297.

[18] C. Bonifazi, A. Letessier-Selvon and E. M. Santos, subm. to Astrop. Phys., astro-ph 0705.1856.

[19] M. Aglietta et. al. for the Pierre Auger Collaboration, "Response of the Pierre Auger Observatory Water Cherenkov Detectors to Muons", Proceedings of the 29th International Cosmic Ray Conference, Pune, India, **7**, 83 (2005)

[20] X. Bertou et. al for the Pierre Auger Collaboration, Nuclear Instruments and Methods in Physics Research **A568** 839 (2006)

[21] The Pierre Auger Collaboration, Nucl. Instr.& Meth. A **523** 50-95 (2004)

[22] A. Filevich et. al, Nucl. Inst. & Meth. **A423**, 69 (1999)

[23] J. Ogwoka Gichaba, "Measurements of Tyvek Reflective Properties for the Pierre Auger Project," University of Missippi Masters Thesis (1998). http://lss.fnal.gov/archive/masters/fermilab-masters-1998-05.pdf

[24] I. Allekotte et. al. for the Pierre Auger Collaboration, "Observation of the Long Term Stability of Water Stations in the Pierre Auger Surface Detector", Proceedings of the 29th International Cosmic Ray Conference, Pune, India, **8**, 287 (2005)

[25] P. Allison et. al. for the Pierre Auger Collaboration, "Observing muon decays in water Cherenkov detectors at the Pierre Auger Observatory", Proceedings of the 29th International Cosmic Ray Conference, Pune, India, **8**, 299 (2005)